INTERLAMINAR AND INTRALAMINAR PROPERTIES OF CARBON SPREAD TOW AND GLASS FIBRE HYBRID COMPOSITES FOR COST SAVING IN THE MASS PRODUCTION OF AUTOMOTIVE COMPONENTS

T. J, Katafiasz[1], L.Iannucci[1], E. S. Greenhalgh[1]

[1]Department of Aeronautics, Imperial College London, Exhibition Road, London SW7 2AZ, UK
First Author Email: tomas.katafiasz11@imperial.ac.uk, Web Page: http://www.imperial.ac.uk

Keywords: fibre hybrid composite, spread tow, thin ply, automotive, interlaminar, intralaminar, shear, short beam, compact tension, thermoset, carbon, glass

Abstract

As the efficiency of the automotive engine shows signs of slow-down and the consumer is becoming more aware of the consequential ecological impact, the industry's need for lighter component materials grows more prominent. Carbon fibre composite materials have been subject to neglect within the consumer automotive industry due to their expense (whereas glass fibre materials have been used favourably over the last few decades [1]). Cost effective composite materials have therefore become an area of interest for the consumer automotive market, where year-on-year engine efficiency performance improvements and monetary savings are integral to company profits.

The purpose of this research is to verify that the use of fibre hybrid composites, where two-stage pseudo-ductile responses can be found [2], [3], are a viable alternative to monolithic structures (which exhibit a more traditional one-stage brittle failure) in interlaminar and intralaminar failure modes. In recent years, there has been much work to understand the tensile response of fibre hybrid composites [2]–[5] but a lack of research in types of failure modes which are more likely within automotive components; these being delamination (interlaminar) and through-thickness tearing (intralaminar); the latter of which most likely occurs at stress concentrations at bolt holes and through-thickness discontinuities.

1. Introduction

The automotive industry is moving towards a lighter and more energy efficient vehicle and in response, research has been undertaken to show that fibre hybrid composites (when less expensive than non-hybrid fibre composites) can exhibit similar if not favourable mechanical properties throughout a range of loading scenarios [6], [7]. There has been considerable interest concerning the tensile properties of carbon/glass fibre composites due to their pseudo-ductile response but little work has been conducted regarding interlaminar or intralaminar failure, which are more indicative of likely failure modes within these components. The interlaminar shear strength can be described as a laminate's resistance to delamination within a ply-stacked composite layup. The intralaminar shear properties (Mode-I) can be described as a laminate's resistance to tearing (Figure 3). See Figure 1 for further clarification of both failure planes (note, since 0º/90º materials are used, the term intralaminar is used to encompass intralaminar and translaminar fracture across the through-thickness plane).

Excerpt from ISBN 978-3-00-053387-7

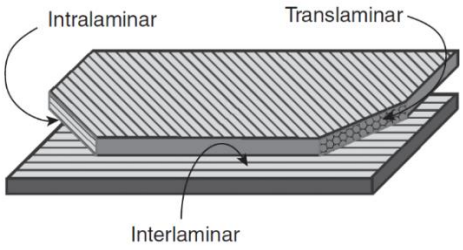

Figure 1. Illustration of translaminar, intralaminar and interlaminar failure planes [8]

The purpose of this research is to further understand the interlaminar and intralaminar properties of spread tow carbon / glass fibre hybrid composites. This particular composite system's viability in the automotive industry is important because favourable material properties can be achieved alongside significant cost savings compared to monolithic carbon composite structures.

2. Materials and Test Standards

To rank and characterise the properties of fibre hybrid composites, monolithic counterparts of the hybrid are to be tested and compared (Table 1).

Table 1. Material data

Name	Fibre Architecture	Fibre Type	Resin Type	Fibre volume fraction
Monolithic carbon	Plain Weave Spread Tow[1]	Toray T700S	MTM57	~55%
Monolithic glass	NCF Biaxial (0°/90°)[2]	S2-Glass	MTM57	~55%
Hybrid	Interlayer fibre hybrid (consisting of [1,2])	Toray T700S / S2-Glass	MTM57	~55%*

*of which 34% carbon, 66% glass

The BS ISO 14130:1998 standard [9] (also known as the 'short-beam' test) is utilised to determine the relative interlaminar shear properties. The test consists of a small 20x10x4mm specimen placed under three loading points as shown in Figure 2. The maximum shear occurs mid-plane and is represented quantitatively by a load drop from the test apparatus (Figure 5).

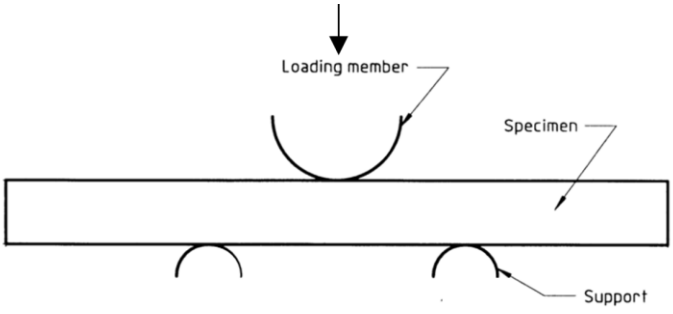

Figure 2. BS ISO 14130:1998 standard 'short-beam' test method load scenario [9]

Excerpt from ISBN 978-3-00-053387-7

The ASTM E1457-13 standard [10] (commonly known as the Compact Tension (CT) test) is used as a basis for determining the intralaminar properties. The test consists of a specimen with two bearing points loaded in tension with a notch initiating through-thickness crack growth (Figure 3). The recommended specimen geometry is utilised and altered to account for the comparatively (to carbon fibre) poorer compression strength that glass fibre composites exhibit. By doing so, an optimised CT design is to be proposed and used to test the materials for intralaminar critical energy release rate.

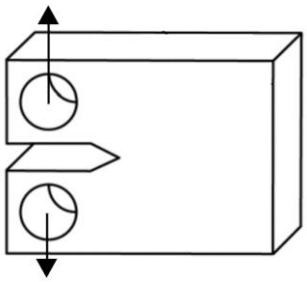

Figure 3. CT specimen loading arrangement [10]

3. Interlaminar Properties

3.1. Manufacture

The three primary material systems being tested are manufactured using an RFI (Resin Film Infusion) technique. A curing cycle ramping to 120˚C and held for one hour is then allowed to cool unaided to room temperature (Figure 4).

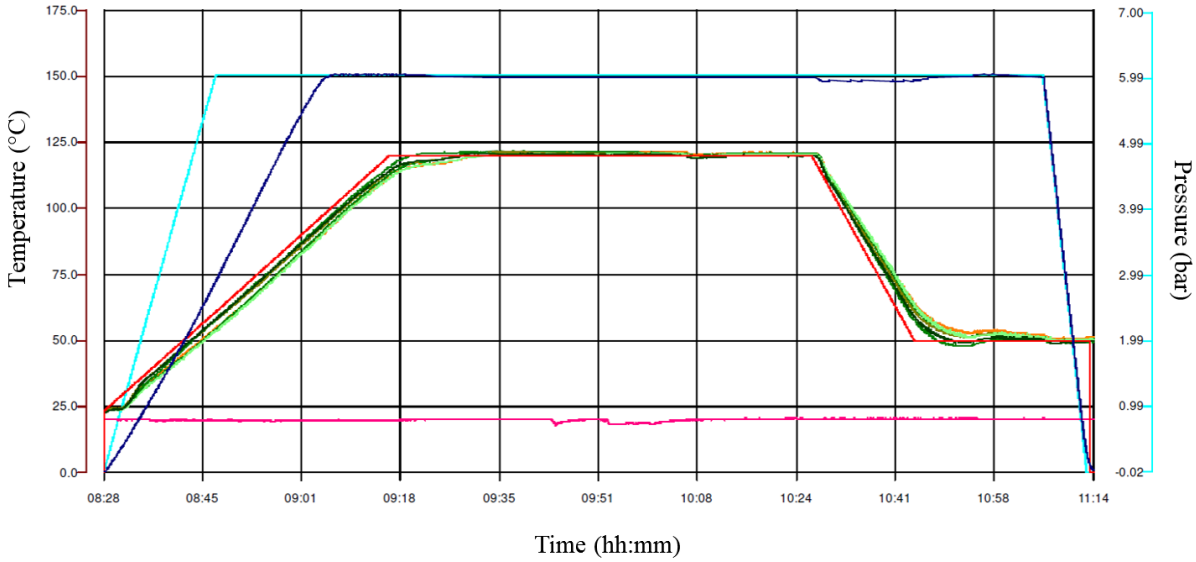

Figure 4. MTM57 3 hour cure cycle (courtesy of Cyctec-Solvay, Heanor, UK)

After curing the panels are NDT (Non-Destructive Testing) C-Scanned at a frequency of 5MHz at a scanning rate of 100mm/s and resolution of 0.5mm within a water bath couplant to check for manufacturing errors such as delaminations, flaws and porosities. The specimens are then cut to size from larger panels using a waterjet cutting machine.

Excerpt from ISBN 978-3-00-053387-7

3.2. Testing and Results

The 'short-beam' test method is tested using an Instron 5969, following the BS ISO 14130:1998 standard [9]. Figure 5 shows typical traces of the interlaminar shear strength of the hybrid, monolithic carbon and monolithic glass. The hybrid and monolithic carbon interlaminar shear strength = 57.1 MPa (CV = 8.90%) and the monolithic glass interlaminar shear strength = 51.8 MPa (CV = 8.71%).

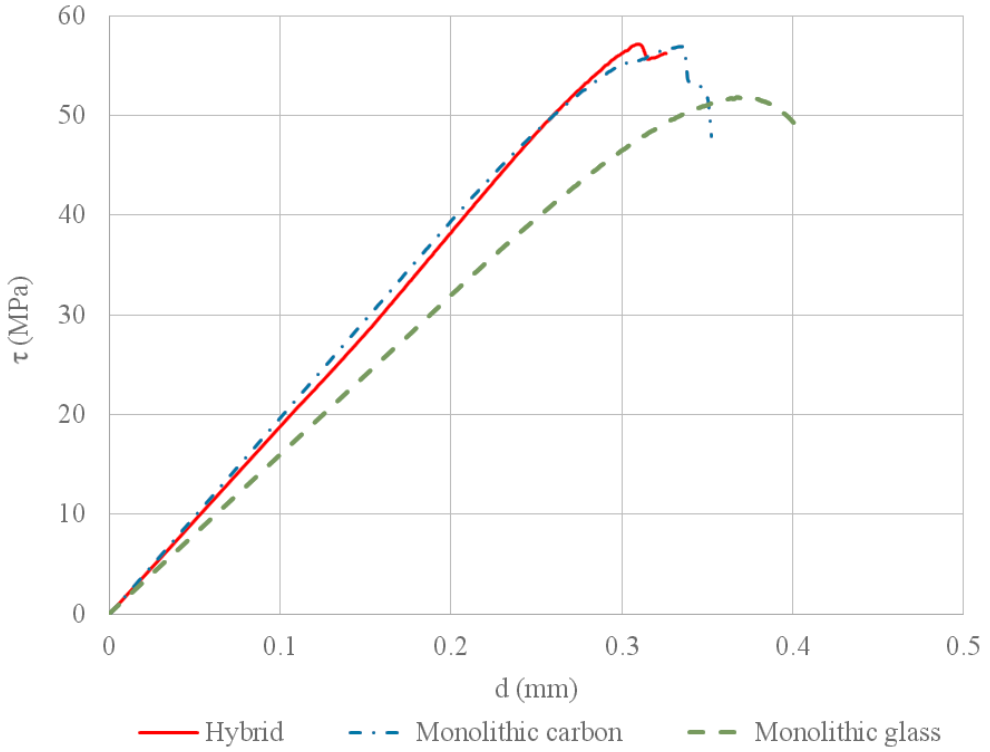

Figure 5. Interlaminar shear strength (τ) vs displacement (d) for the hybrid, monolithic carbon, and monolithic glass

4. Intralaminar Properties

4.1. Specimen Optimisation through Finite Element Modelling

Two finite element models are run under Abaqus 6.14 Windows x86 using the linear static module to determine the stresses, and the normal modes eingenvalue module to determine the critical buckling loads of the CT specimen. The various iterations of the model are split through the thickness, comprising of continuum shell elements (SC8R) and cohesive elements (COH3D8). The continuum shell elements are assigned the monolithic glass material properties (from tensile [11], compressive [12] and short-beam shear [9] tests) using the Abaqus composite material property for each ply (where one element through-thickness contains two plies, and each ply with three integration points). The cohesive elements are assigned the pure resin properties (from tensile [13] and compressive [14] tests) so as to capture any delaminations between neighbouring plies.

Preliminary experimental tests and FE models show that buckling failure and premature compressive failure occur at the rear of the CT specimen for the monolithic glass when using the ASTM E1457-13 standard [10] CT specimen geometry (Figure 6). It is therefore necessary that the design should be optimised to account and mitigate these invalid modes of failure.

Excerpt from ISBN 978-3-00-053387-7

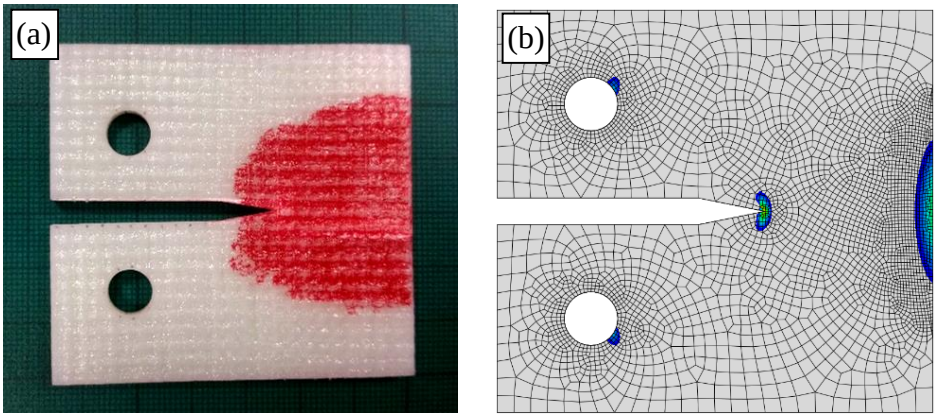

Figure 6. ASTM E1457-13 specimen geometry: a) Invalid experimental test (red dye to expose crack) (b) FE model - MSTRN (maximum strain) failure

An optimised specimen geometry has been developed through iterations of linear static stress and eigenvalue buckling models (Figure 7). To disperse the compressive stress concentrations a curvature at the rear of the specimen is incorporated. The thickness of the crack growth area is reduced by cutting an area into the dry fibres prior to curing therefore increasing the critical buckling load relative to the critical fracture load, allowing crack growth without buckling.

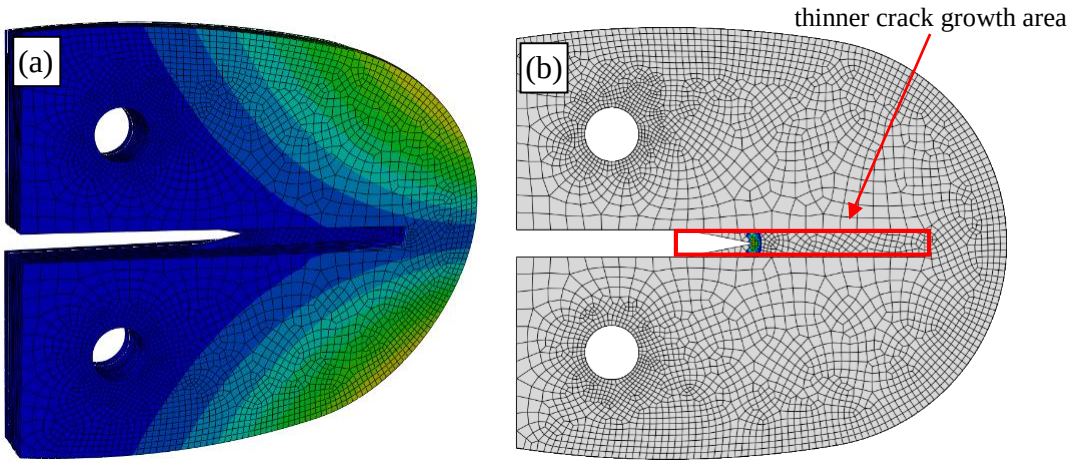

Figure 7. Optimised CT specimen geometry: a) Eigenvalue first buckling mode (b) FE Model - MSTRN failure

4.2. Manufacture

The specimens for the intralaminar testing follow the same sequence of manufacture as the interlaminar specimens, where RFI, C-scanning and waterjet cutting is employed. There is however a variation in the layup sequence and some cutting of the dry fibres prior to curing around the thinner crack growth region (Figure 7). Three multiple-ply stacks are laid-up using resin film and dry fibres, with rectangular cuts made on the outer two, the same size of the crack growth region (Figure 8). Rectangular PTFE inserts with the same thickness as the cured stack thickness are then placed into the cut regions to prohibit resin flow into the region. The ply stacks are then consolidated in a vacuum table overnight and cured together using the standard RFI curing cycle for the MTM57 resin (Figure 4).

Excerpt from ISBN 978-3-00-053387-7

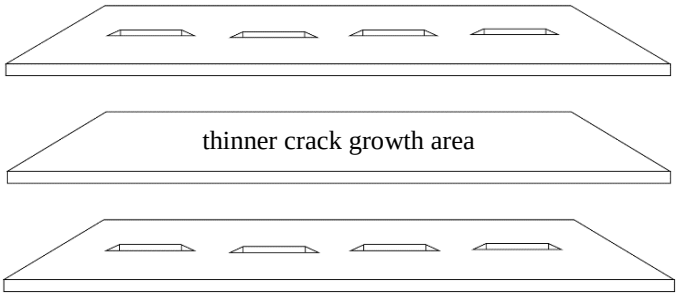

Figure 8. Exploded ply stacking diagram for optimised CT specimen panel

The cured panels are then cut into the desired specimen shape using a waterjet cutting machine and the PTFE inserts removed. The notch tip is cut using a circular diamond-tip saw blade to ensure an appropriately sharp crack initiation site (Figure 9).

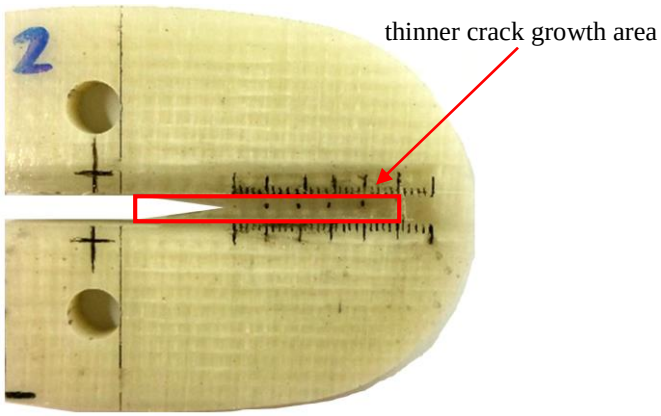

Figure 9. Cured and cut optimised CT specimen pre-test

4.3. Testing

The CT test is loaded as shown in Figure 3 and carried out under room temperature using an Instron 5969 at a constant rate of 0.5mm/min in tension, where the crosshead displacement (mm), load (N) and time (s) is recorded. Video capture is also employed to capture the crack growth (mm) and the crosshead displacement (mm) to eliminate any instrumentation compliance and is done so using an Imetrum optical strain video system. A backlight is used to show clear crack growth through the specimen thickness.

Data is captured in both the Intron and Imetrum system at 10 points per second and correlated using the time recorded at each point. By doing so, the load vs displacement curves are plotted and instrumentation compliance is not captured.

4.4. Data Reduction

A Modified Compliance Method (MCC) approach [15] is used to calculate the critical energy release rate at various crack lengths. The following formula is used to determine the critical energy release rate G_{IC} (J/m^2) of the material, where P_c = load (N), t = specimen thickness at crack (m), dC/da = change in specimen elastic compliance at given crack length (m/N).

Excerpt from ISBN 978-3-00-053387-7

$$G_{IC} = \frac{P_c^{\,2}}{2t} \cdot \frac{dC}{da}$$

The dC/da curve is calculated numerically by plotting points of the elastic compliance (C) over a range of crack lengths (a) in linear static FE models (Figure 10). The compliance of the FE model at a 0mm crack growth is 0.989 that of the experimental tests. The line of best fit is found as an exponential equation and is differentiated to give dC/da as a function of crack length. To calculate the critical energy release rate, points are taken from the load vs displacement curves at load drops correlated to the corresponding crack length events in the video capture.

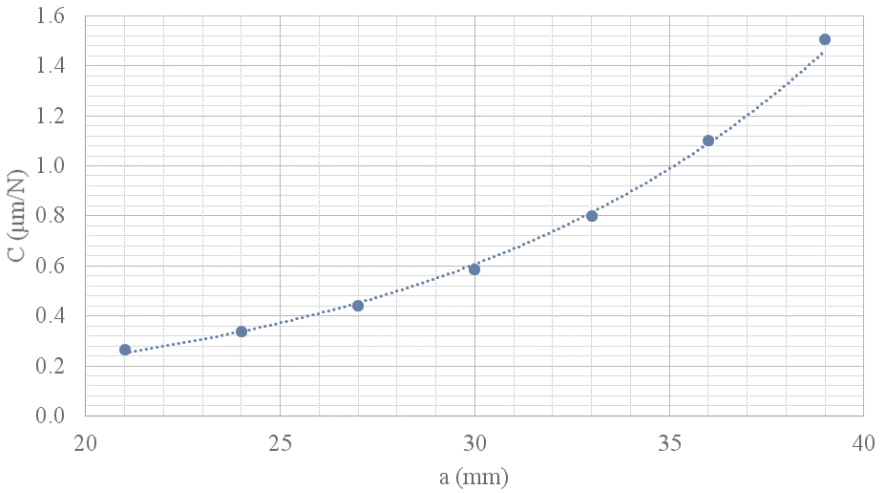

Figure 10. Elastic compliance (C) vs crack length (a) from linear static FE model

4.5. Results

Figure 11 shows for the monolithic glass (0°/90° properties), the initiation critical energy release rate = 131.9 kJ/m^2 (CV = 0.004%) and the propagation critical energy release rate = 154.2 kJ/m^2 (CV = 8.58%).

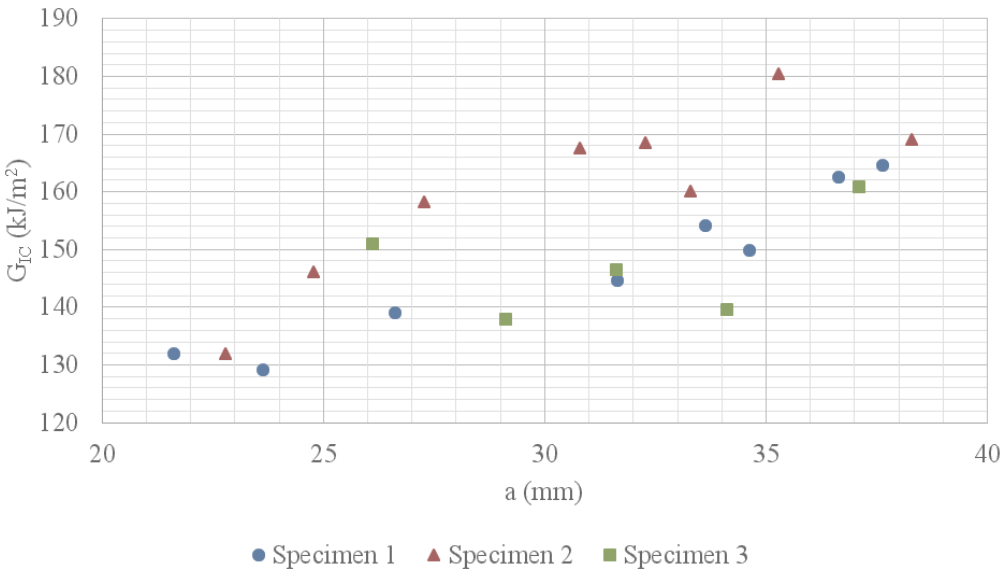

Figure 11. Critical energy release rate (G_{IC}) vs crack length (a) for monolithic glass

Excerpt from ISBN 978-3-00-053387-7

5. Conclusions

- Interlaminar testing shows that possible cost savings can be made for delamination resistance in automotive components where the interlaminar shear strength of the hybrid composite is comparable to the monolithic carbon.

- The intralaminar testing using the optimised CT specimen design has shown that repeatable and accurate values of the critical energy release rate can be achieved. The monolithic carbon and hybrid intralaminar critical energy release rates are to be presented and discussed at the ECCM17 conference in June 2016.

Acknowledgements

Funding from AMSCI DATACOMP and materials from Sigmatex and Cytec-Solvay is acknowledged.

References

[1] A. Erber, "Material Innovations and Design Concepts for Thermoplastic Composites," in *4th International Congress Automotive Composites*, 2013.
[2] M. Jalalvand, G. Czél, and M. R. Wisnom, "Numerical modelling of the damage modes in UD thin carbon/glass hybrid laminates," *Compos. Sci. Technol.*, vol. 94, pp. 39–47, Apr. 2014.
[3] G. Czél, M. Jalalvand, and M. R. Wisnom, "Demonstration of pseudo-ductility in unidirectional hybrid composites made of discontinuous carbon/epoxy and continuous glass/epoxy plies," *Compos. Part A Appl. Sci. Manuf.*, vol. 72, pp. 75–84, 2015.
[4] H. Yu, M. L. Longana, M. Jalalvand, M. R. Wisnom, and K. D. Potter, "Pseudo-ductility in intermingled carbon/glass hybrid composites with highly aligned discontinuous fibres," *Compos. Part A Appl. Sci. Manuf.*, vol. 73, pp. 35–44, 2015.
[5] M. Jalalvand, G. Czél, and M. R. Wisnom, "Damage analysis of pseudo-ductile thin-ply UD hybrid composites - a new analytical method," *Compos. Part A Appl. Sci. Manuf.*, vol. submitted, pp. 83–93, 2014.
[6] C. Zweben, "Tensile strength of hybrid composites," *J. Mater. Sci.*, vol. 12, pp. 1325–1337, 1977.
[7] Y. Swolfs, L. Gorbatikh, and I. Verpoest, "Fibre hybridisation in polymer composites: A review," *Compos. Part A Appl. Sci. Manuf.*, vol. 67, pp. 181–200, Sep. 2014.
[8] E. S. Greenhalgh, *Failure analysis and fractography of polymer composites*. Cambridge, UK: Woodhead Publishing Ltd., 2009.
[9] BSi, "BS ISO 14130:1998 Fibre-reinforced plastic composites — Determination of apparent interlaminar shear strength by short-beam method," vol. 3. 1998.
[10] ASTM, "ASTM E1457-13 Standard Test Method for Measurement of Creep Crack Growth Times and Rates in Metals," *ASTM E1457*. 2013.
[11] BSi, "BS ISO 527-4: 1997 Plastics — Determination of tensile properties - Part 4: Test conditions for isotropic and orthotropic fibre-reinforced plastic composites." 1997.
[12] J. Haeberle and F. L. Matthews, "Studies on compressive failure in unidirectional CFRP using improved test method," London, 1990.
[13] BSi, "BS ISO 527-2:2012 Determination of tensile properties Part 2 : Test conditions for moulding and extrusion plastics," 2012.
[14] BSi, "BS ISO 604:2003 Plastics — Determination of compressive properties," vol. 3, 2003.
[15] M. J. Laffan, S. T. Pinho, P. Robinson, and L. Iannucci, "Measurement of the in situ ply fracture toughness associated with mode I fibre tensile failure in FRP. Part I: Data reduction," *Compos. Sci. Technol.*, vol. 70, no. 4, pp. 606–613, 2010.

Excerpt from ISBN 978-3-00-053387-7